Int. J. Solids Structures Vol. 21, No. 11, pp. 1131–1145, 1985
Printed in Great Britain.

0020-7683/85 $3.00 + .00

A CLASS OF PLASTIC CONSTITUTIVE EQUATION WITH VERTEX EFFECT—III. APPLICATIONS TO CALCULATION OF FLD OF METAL SHEETS

MANABU GOTOH
Department of Precision Engineering, Gifu University, Yanagido 1-1, Gifu-City, 501-11, Japan

(*Received* 3 *October* 1983)

Abstract—The constitutive equation proposed in the previous papers of this series is applied to theoretical determination of FLD (forming limit-strain diagram) of metal sheets. The condition of localized necking due to Stören and Rice is derived by making use of this constitutive equation and the formula of limit-strain is obtained on the basis of this localized necking condition as the breakage condition. The formula is also formulated for the case where normal anisotropy is taken into account by introducing $\bar{r}$-value and/or $\bar{X}$-value. Then FLDs of several metal sheets are determined and compared with the corresponding experimental data to confirm a fairly good agreement. It is also emphasized that the value of Θ_0 (= the half angle of the pointwise-vertexed subsequent loading surface at the loading point) is within the range 70°–89° even at the onset of breakage throughout all materials tested here, and therefore it would be very difficult to check experimentally the vertex formation by the usual method of determination of subsequent yield surface at far smaller strain level as reported so far.

1. INTRODUCTION

In the previous two papers of this series of work[1, 2], a class of plastic constitutive equations with vertex effect was proposed and developed, and its simplest form was examined by several numerical calculations. In this paper (Part III), this constitutive equation is applied to theoretical determination of the forming limit diagram (FLD) of several ductile metal sheets specifically for the case where proportional loading or straining is applied. And comparison of the theoretical results with the experimental results is also presented.

In the past, because of its practical importance in press-working processes, the forming limit (breakage) strain of ductible metal sheets has been investigated both experimentally and theoretically by many workers. For example, Swift[3] proposed an idea to determine it for the case of biaxial stretching, which is now well known as Swift instability condition. Hill[4] also proposed the similar idea and called it as the condition of diffuse necking. Diffuse necking is the in-plane necking phenomenon which occurs in a sheet strip under uniaxial tension (say) at the maximum load, and is now understood as a bifurcation phenomenon which precedes breakage. He also proposed another instability condition—local necking condition—which is accompanied with severe local thinning along a narrow band with width of about sheet thickness and thus leads immediate breakage. However, his local necking condition makes sense only for positive strain ratio n for a proportional loading, where $n = \epsilon_2/\epsilon_1$; ϵ_1, ϵ_2 = major and minor planar strains. Therefore, the theoretical FLD for proportional loadings was determined on the basis of two instability conditions—i.e. diffuse necking condition for $n > 0$ and local necking condition for $n < 0$. This method is, of course, not very exact even in a logical sense because diffuse necking does not mean breakage. Rather recently Marciniak and Kuczynski[5] proposed to introduce the idea of initial imperfection of the material to overcome this difficulty (M–K theory or model). Since then this model was used to determine FLD for $n > 0$[6–8]. However, FLD determined by this model is apt to show a too steep upward slope over the range from $n = 0$ to $n = 1$, and evaluation of the value of the imperfection factor f is not necessarily clear and appropriate. Moreover, FLD for $n < 0$ is not easily determined, and even FLD for $n \geqq 0$ must be obtained by a numerical method. Stören and Rice[9] proposed a theoretical method to determine

the local necking condition for a perfect sheet (S–R theory or model), which is now understood to be a condition for bifurcation in a local mode similar to the shear-band-type bifurcation in a plane-strain block. Their theory requires the plastic constitutive equation to have one-to-one correspondence between plastic strain increment $d\boldsymbol{\epsilon}^p$ and stress increment $d\boldsymbol{\sigma}$ to get reasonable limiting strain in the range of $n > 0$. They used the incremental form of J_2-deformation theory in its hypoelastic version. However, a comparison of their theory with the experiments verifies a necessity of improvement of the constitutive equation.

Here we make use of our plastic constitutive equation to determine FLDs of several commercial metal sheets for proportional loadings adopting the S–R's local necking condition as the breakage condition. Theoretical FLDs for *non*proportional loadings without unloading and theoretical secondary FLDs (FLDs of prestrained metal sheets) will be presented in the following work of this series (Part IV).

2. CONSTITUTIVE EQUATION

The constitutive equation used here has the following expression which was developed and discussed in Part II[2]:

$$\begin{aligned} d\mathbf{e} &= (1/2G^*)\,\mathring{d}\mathbf{T} + (b/2\bar{\sigma}\,h_0^*)\mathbf{T}\,\overline{d\sigma}, \\ \operatorname{tr} d\boldsymbol{\epsilon} &= (1/3K)\operatorname{tr} d\boldsymbol{\sigma}, \end{aligned} \tag{1}$$

where incompressible plasticity is assumed, and

$$\begin{aligned} d\boldsymbol{\epsilon} &= \text{strain increment}, \\ d\mathbf{e} &= d\boldsymbol{\epsilon} - (1/3)\operatorname{tr} d\boldsymbol{\epsilon}; \qquad (\operatorname{tr} = \text{trace symbol}), \\ d\boldsymbol{\sigma} &= \text{increment of Cauchy stress } \boldsymbol{\sigma}, \\ \mathbf{T} &= \boldsymbol{\sigma} - (1/3)\operatorname{tr}\boldsymbol{\sigma}, \\ \mathring{d}\mathbf{T} &= d\mathbf{T} - d\boldsymbol{\omega}\mathbf{T} + \mathbf{T}\,d\boldsymbol{\omega} = \text{Jaumann increment of } \mathbf{T}, \\ d\boldsymbol{\omega} &= \text{increment of rigid-body rotation}, \\ \bar{\sigma} &= \sqrt{3/2}\,[\operatorname{tr}(\mathbf{T}^2)]^{1/2}, \\ \overline{d\sigma} &= \sqrt{3/2}\,[\operatorname{tr}(\mathring{d}\mathbf{T}^2)]^{1/2}, \qquad (\neq d\bar{\sigma}) \end{aligned} \tag{2}$$

$$\begin{aligned} 1/G^* &= 1/G + \langle P(\Theta)\rangle/H_0 \\ 1/h_0^* &= \langle P(\Theta)\rangle/h_0, \end{aligned} \tag{3}$$

$$P(\Theta) = a + b\cos\Theta, \tag{4}$$

$$\langle P\rangle = P \quad \text{for} \quad P > 0, \qquad \langle P\rangle = 0 \quad \text{for} \quad P \leqq 0, \tag{5}$$

$$\cos\Theta = \operatorname{tr}(\mathbf{T}\,\mathring{d}\mathbf{T})/\{[\operatorname{tr}(\mathbf{T}^2)][\operatorname{tr}(\mathring{d}\mathbf{T}^2)]\}^{1/2}, \tag{6}$$

$$\begin{aligned} a &= h_0/H_0 = \cos\Theta_0/(1+\cos\Theta_0), \\ b &= 1 - a, \end{aligned} \tag{7}$$

$$h_0 = (1/3)\cdot[\text{slope of } (\bar{\sigma}\text{–}\epsilon) \text{ curve for a proportional loading}], \tag{8}$$

$$\epsilon = \int \overline{d\epsilon^p}; \qquad \overline{d\epsilon^p} = \sqrt{2/3}\,[\operatorname{tr}(d\mathbf{e}^{p2})]^{1/2}, \tag{9}$$

$$d\mathbf{e}^p = \text{plastic strain increment},$$

and the half angle Θ_0 of the cone of the subsequent loading surface at the loading point

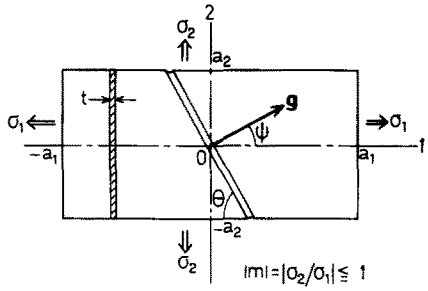

Fig. 1. An element of sheet metal with localized necking band.

is given as

$$\Theta_0 = (\pi/2) - \rho\epsilon^2, \tag{10}$$

where ρ is a material constant. If $\rho = 0$, then Θ_0 is consistently equal to $(\pi/2)$, which means that no vertex forms with deformation and eqn (1) reduces to the classical J_2-flow theory. h_0 and H_0 are the instantaneous work-hardening and vertex-hardening rate, respectively. G and K are the elastic shear-rigidity and bulk modulus, respectively. If Θ for subsequent $\mathring{d}T$ satisfiies the following inequality,

$$\begin{aligned} &0 \leqq \Theta < \Theta_{\max}, \\ &\Theta_{\max} = \cos^{-1}(-a/b), \end{aligned} \tag{11}$$

then plastic deformation continues for this stress increment. The inverse relation of eqn (1) is also discussed in detail in Part II.

Now let us consider a rectangular element of metal sheet with thickness t subjected to biaxial stretching as illustrated in Fig. 1. σ_1 is the major principal stress and σ_2 is the minor one, respectively, where $\sigma_1 > 0$ and $|m| \leqq 1$, $m = \sigma_2/\sigma_1$ (stress ratio). Here plane stress state is assumed. Introducing the following denotations:

$$\begin{aligned} &\mathring{T} = dT/\overline{d\sigma}, \\ &\dot{\epsilon} = d\epsilon/\overline{d\epsilon}; \qquad \dot{\bar{\epsilon}} = d\epsilon/\overline{d\sigma}, \\ &\overline{d\epsilon} = \sqrt{2/3}\,[\mathrm{tr}\,(d\epsilon^2)]^{1/2}, \end{aligned} \tag{12}$$

the constitutive equation reduces to the following expressions:

$$\begin{aligned} \dot{\bar{\epsilon}}_{11} = {} & (1/12\bar{\sigma}H_0)b[2(2\sigma_1 - \sigma_2)\mathring{\sigma}_1^2 - (2\sigma_2 - \sigma_1)\mathring{\sigma}_2^2 + (5\sigma_2 - 4\sigma_1)\mathring{\sigma}_1\mathring{\sigma}_2] \\ & + [(1/3G') + (1/12\bar{\sigma}^2h_0)b^2(2\sigma_1 - \sigma_2)^2]\mathring{\sigma}_1 + [-(1/6G') \\ & + (1/12\bar{\sigma}^2h_0)b^2(2\sigma_1 - \sigma_2)(2\sigma_2 - \sigma_1)]\mathring{\sigma}_2 + (1/6\bar{\sigma}h_0)ab(2\sigma_1 - \sigma_2), \end{aligned} \tag{13}$$

$$\begin{aligned} \dot{\bar{\epsilon}}_{22} = {} & (1/12\bar{\sigma}H_0)b\{2(2\sigma_2 - \sigma_1)\mathring{\sigma}_2^2 - (2\sigma_1 - \sigma_2)\mathring{\sigma}_1^2 + (5\sigma_1 - 4\sigma_2)\mathring{\sigma}_2\mathring{\sigma}_1 \\ & + [(1/3G') + (1/12\bar{\sigma}^2h_0)b^2(2\sigma_2 - \sigma_1)^2]\mathring{\sigma}_2 + [-(1/6G') \\ & + (1/12\bar{\sigma}^2h_0)b^2(2\sigma_2 - \sigma_1)(2\sigma_1 - \sigma_2)]\mathring{\sigma}_1 + (1/6\bar{\sigma}h_0)ab(2\sigma_2 - \sigma_1), \end{aligned} \tag{14}$$

$$\dot{\bar{\epsilon}}_{12} = (1/4\bar{\sigma}H_0)b[(2\sigma_1 - \sigma_2)\mathring{\sigma}_1 + (2\sigma_2 - \sigma_1)\mathring{\sigma}_2]\mathring{\tau}_{12} + (1/2G')\mathring{\tau}_{12}, \tag{15}$$

where plastic loading state is assumed, and

$$\begin{aligned} &\overline{d\sigma} = (\mathring{d}\sigma_1^2 + \mathring{d}\sigma_2^2 - \mathring{d}\sigma_1\,\mathring{d}\sigma_2 + 3\,\mathring{d}\tau_{12}^2)^{1/2}, \\ &\bar{\sigma} = (\sigma_1^2 + \sigma_2^2 - \sigma_1\sigma_2)^{1/2}, \end{aligned} \tag{16}$$

and $1/G' = (1/G) + (h_0/H_0^2)$, and the existence of $\mathring{\tau}_{12}$ is allowed at the moment under consideration, though τ_{12} is set equal to 0.

3. LOCAL NECKING CONDITION

Suppose that, after proportional deformation of a certain magnitude, discontinuities in velocity gradient $\mathbf{v}_{,i}$ and stress rate $\mathring{\boldsymbol{\sigma}}$ have taken place along a narrow band of breadth of about sheet thickness as illustrated in Fig. 1. This is the so-called localized bifurcation band[9]. We denote the unit normal vector to this band by $\mathbf{g}(g_1, g_2)$. Marking superfixes $+$ and $-$ to the quantities outside and inside the local necking band, respectively, we denote the discontinuity between them by $\Delta X = X^+ - X^-$, say. Then we obtain the following relations from eqns (13)–(15):

$$\Delta \begin{pmatrix} \mathring{\sigma}_1 \\ \mathring{\sigma}_2 \\ \mathring{\tau}_{12} \end{pmatrix} = \begin{pmatrix} a_{11} & a_{12} & 0 \\ a_{21} & a_{22} & 0 \\ a_{31} & a_{32} & a_{33} \end{pmatrix} \Delta \begin{pmatrix} v_{1,1} \\ v_{2,2} \\ (v_{1,2} + v_{2,1}) \end{pmatrix}, \tag{17}$$

where $v_{i,j} = \mathrm{d}(\partial u_i/\partial x_j)/\overline{\mathrm{d}\sigma}$, i.e. $\mathbf{v} = \mathrm{d}\mathbf{u}/\overline{\mathrm{d}\sigma}$, where $\mathbf{u}$ denotes displacement vector, and

$$a_{11} = a_{22}^*/D^*, \quad a_{12} = -a_{12}^*/D^*, \quad a_{21} = -a_{21}^*/D^*,$$
$$a_{22} = a_{11}^*/D^*, \quad a_{31} = (-a_{31}^* a_{22}^* + a_{32}^* a_{21}^*)/(a_{33}^* D^*), \tag{18}$$
$$a_{32} = (a_{31}^* a_{12}^* - a_{32}^* a_{11}^*)/(a_{33}^* D^*), \quad a_{33} = 1/(2a_{33}^*),$$

$$D^* = a_{11}^* a_{22}^* - a_{12}^* a_{21}^*, \quad a_{11}^* = 4\tilde{a}_1 \mathring{\sigma}_1^* + \tilde{a}_3 \mathring{\sigma}_2^* + \tilde{b}_1, \quad a_{12}^* = -2\tilde{a}_2 \mathring{\sigma}_2^* + \tilde{a}_3 \mathring{\sigma}_1^* + \tilde{b}_2,$$

$$a_{21}^* = -2\tilde{a}_1 \mathring{\sigma}_1^* + \tilde{a}_4 \mathring{\sigma}_2^* + \tilde{b}_2, \quad a_{22}^* = 4\tilde{a}_2 \mathring{\sigma}_2^* + \tilde{a}_4 \mathring{\sigma}_1^* + \tilde{b}_3, \quad a_{31}^* = \mathrm{d}_1 \mathring{\tau}_{12}^*, \tag{19}$$

$$a_{32}^* = \mathrm{d}_2 \mathring{\tau}_{12}^*, \quad a_{33}^* = (1/2G') + \mathrm{d}_1 \mathring{\sigma}_1^* + \mathrm{d}_2 \mathring{\sigma}_2^*,$$

$$\mathring{\sigma}_1^* = (\mathring{\sigma}_1^+ + \mathring{\sigma}_1^-)/2, \quad \mathring{\sigma}_2^* = (\mathring{\sigma}_2^+ + \mathring{\sigma}_2^-)/2, \quad \mathring{\tau}_{12}^* = (\mathring{\tau}_{12}^+ + \mathring{\tau}_{12}^-)/2, \tag{20}$$

$$\tilde{a}_1 = h_1 \sigma_1', \quad \tilde{a}_2 = h_1 \sigma_2', \quad \tilde{a}_3 = h_1(2\sigma_2' - \sigma_1'), \quad \tilde{a}_4 = h_1(2\sigma_1' - \sigma_2');$$

$$\tilde{b}_1 = (1/3G') + h_2 \sigma_1'^2, \quad \tilde{b}_2 = -(1/6G') + h_2 \sigma_1' \sigma_2', \tag{21}$$

$$\tilde{b}_3 = (1/3G') + h_2 \sigma_2'^2, \quad \mathrm{d}_1 = 3\tilde{a}_1, \quad \mathrm{d}_2 = 3\tilde{a}_2; \quad \sigma_i' = T_i,$$

$$h_1 = b/(4\bar{\sigma} H_0), \quad h_2 = 3b^2/(4\bar{\sigma}^2 h_0). \tag{22}$$

On the other hand, we know the following relations which are directly derived from the relation between nominal stress rate $\dot{\mathbf{s}} = \mathrm{d}\mathbf{s}/\overline{\mathrm{d}\sigma}$ and Cauchy stress rate $\mathring{\boldsymbol{\sigma}}$, where $\mathbf{s}$ = nominal stress:

$$\Delta \dot{s}_{11} = \Delta \mathring{\sigma}_1 - \sigma_1 \Delta v_{1,1}, \quad \Delta \dot{s}_{12} = \Delta \mathring{\tau}_{12} - \hat{\sigma} \Delta v_{1,2} + \hat{\tau} \Delta v_{2,1},$$
$$\Delta \dot{s}_{21} = \Delta \mathring{\tau}_{21} - \hat{\tau} \Delta v_{1,2} - \hat{\sigma} \Delta v_{2,1}, \quad \Delta \dot{s}_{22} = \Delta \mathring{\sigma}_2 - \sigma_2 \Delta v_{2,2} \tag{23}$$

where $\hat{\sigma} = (\sigma_1 + \sigma_2)/2$ and $\hat{\tau} = (\sigma_1 - \sigma_2)/2$.

Now we set as follows:

$$\Delta v_{i,j} = \gamma_i g_j, \quad (i, j = 1, 2), \tag{24}$$

where $\boldsymbol{\gamma} = (\gamma_1, \gamma_2)$ is the infinitesimal shear along the local neck band. Then we obtain the following relations from eqns (23), (24) and (17):

$$\Delta \dot{s}_{11} = \gamma_1(a_{11} - \sigma_1) g_1 + \gamma_2 a_{12} g_2,$$
$$\Delta \dot{s}_{12} = \gamma_1\{a_{31} g_1 + (a_{33} - \hat{\sigma}) g_2\} + \gamma_2[(a_{33} + \hat{\tau}) g_1 + a_{32} g_2],$$
$$\Delta \dot{s}_{21} = \gamma_1\{a_{31} g_1 + (a_{33} - \hat{\tau}) g_2\} + \gamma_2[(a_{33} - \hat{\sigma}) g_1 + a_{32} g_2] \tag{25}$$
$$\Delta \dot{s}_{22} = \gamma_1 a_{21} g_1 + \gamma_2(a_{22} - \sigma_2) g_2.$$

The balance equation across the local neck band is written as follows:

$$\Delta \dot{s}_{ji} g_j = 0. \tag{26}$$

From this equation together with eqn (25), we obtain the following two equations:

$$\begin{aligned}
&\gamma_1[(a_{11} - \sigma_1)g_1^2 + a_{31}g_1g_2 + (a_{33} - \hat{\tau})g_2^2] + \gamma_2[(a_{12} + a_{33} - \hat{\sigma})g_1g_2 + a_{32}g_2^2] = 0,\\
&\gamma_1[a_{31}g_1^2 + (a_{21} + a_{33} - \hat{\sigma})g_1g_2] + \gamma_2[(a_{33} + \hat{\tau})g_1^2 + a_{32}g_1g_2 + (a_{22} - \sigma_2)g_2^2] = 0.
\end{aligned} \tag{27}$$

This is a system of homogeneous linear equations with respect to γ_1 and γ_2.

As we understand from eqn (24), the condition for the onset of local necking is equivalent to that for the existence of non-zero $\boldsymbol{\gamma}(\gamma_1, \gamma_2)$. For that, the determinant of the coefficient matrix with respect to (γ_1, γ_2) should be equal to 0. Therefore we obtain the following equation as the condition for the onset of local necking type bifurcation or breakage:

$$\begin{aligned}
&(a_{11} - \sigma_1)(a_{33} + \hat{\tau})g_1^4 + \{-a_{31}(a_{12} - \sigma_1) + a_{32}(a_{11} - \sigma_1)\}g_1^3g_2\\
&\quad + [(a_{11} - \sigma_1)(a_{22} - \sigma_2) + (a_{33}^2 - \hat{\tau}^2)\\
&\quad - (a_{12} + a_{33} - \hat{\sigma})(a_{21} + a_{33} - \hat{\sigma})]g_1^2g_2^2\\
&\quad + [a_{31}(a_{22} - \sigma_2) - a_{32}(a_{21} - \sigma_2)]g_1g_2^3 + (a_{22} - \sigma_2)(a_{33} - \hat{\tau})g_2^4 = 0.
\end{aligned} \tag{28}$$

This is a fourth-order algebraic equation with respect to (g_1/g_2). If this equation captures a real root, then a localized necking band, or two such bands because of symmetry, will form along the direction whose unit normal vector is $\mathbf{g}$, and the sheet will break along the band.

For proportional loading, the externally controlled $\mathring{\tau}_{12}^{+}$ is always kept 0. In this case, in eqn (19), $a_{31}^* = a_{32}^* = 0$, and thus for eqn (18) $a_{31} = a_{32} = 0$. Therefore eqn (28) reduces to the following expression:

$$\begin{aligned}
&(a_{11} - \sigma_1)(a_{33} + \hat{\tau})g_1^4 + [(a_{11} - \sigma_1)(a_{22} - \sigma_2) + (a_{33}^2 - \hat{\tau}^2)\\
&\qquad - (a_{12} + a_{33} - \hat{\sigma})(a_{21} + a_{33} - \hat{\sigma})]g_1^2g_2^2 + (a_{22} - \sigma_2)(a_{33} - \hat{\tau})g_2^4 = 0.
\end{aligned} \tag{29}$$

Denoting the stress ratio by m as follows,

$$m = \sigma_2/\sigma_1 = \mathring{\sigma}_1^*/\mathring{\sigma}_2^* \qquad \text{(proportional loading)}, \tag{30}$$

we finally obtain the governing equation expressed in eqn (29) in the following expressions:

$$Ag_1^4 + Cg_1^2g_2^2 + Eg_2^4 = 0, \tag{31}$$

$$\begin{aligned}
&A = (a_{11} - \sigma_1)(a_{33} + \hat{\tau}), \qquad E = (a_{22} - \sigma_2)(a_{33} - \hat{\tau}),\\
&C = (a_{11} - \sigma_1)(a_{22} - \sigma_2) + (a_{33}^2 - \hat{\tau}^2) - (a_{12} + a_{33} - \hat{\sigma})^2,
\end{aligned} \tag{32}$$

$$\begin{aligned}
&a_{11} = (1/3D^*)\{(1/G) + (1/H_0) + [b(1 - 2m)^2/4h_0(1 - m + m^2)]\},\\
&a_{22} = (1/3D^*)\{(1/G) + (1/H_0) + [b(2 - m)^2/4h_0(1 - m + m^2)]\},\\
&a_{12} = a_{21} = (1/6D^*)[(1/G) + (1/H_0) + \{b(1 - 2m)(2 - m)/2h_0(1 - m + m^2)\}],\\
&a_{33} = 1/[(1/G) + (1/H_0)]; \qquad D^* = (1/12)[(1/G) + (1/h_0)][(1/G) + (1/H_0)]
\end{aligned} \tag{33}$$

If $a_2 < a_1$ in Fig. 1, then generally

$$0 < a_2/a_1 < g_1/g_2 \tag{34}$$

holds. Therefore $E \neq 0$ is met throughout deformation, because eqn (31) possesses the root of $g_1/g_2 = 0$ if $E = 0$. And it is easily found that at early stage of deformation $E > 0$ is met. Therefore E is always positive. Then, as easily found, eqn (31) possesses the real root(s) if

$$A = 0, \quad \text{or} \quad A \geqq 0 \quad \text{and} \quad C \leqq -2\sqrt{AE} \tag{35}$$

is satisfied. Therefore the critical condition for the onset of local necking or breakage is given by the following equations:

$$A = 0; \quad \text{or} \quad C = -2\sqrt{AE}. \tag{36}$$

At early stage of deformation, $A > 0$ and $C > -2\sqrt{AE}$ hold. When deformation goes, either of the two equations in eqn (36) is met at a certain stage of deformation and the sheet breaks. Which one of the two in eqn (36) precedes the other depends on the stress ratio m, where $|m| \leqq 1$. There exists the value of m, m_0 say, for which both of the two equations in eqn (36) are satified at the same time. It is easily found that m_0 is the real root of the following equation:

$$(1 - m_0)\{4(1 - m_0 + m_0^2) + \tilde{h}(2m_0 - 1)(2m_0 + 5) - G^*(1 - m_0) \times [4(1 - m_0 + m_0^2) + \tilde{h}(2m_0 - 1)^2]^2/2(1 - m_0 + m_0^2)\} = 0, \tag{37}$$

where

$$\tilde{h} = a_{33}[(1/h_0) - (1/H_0)], \qquad G^* = 1/\{a_{33}[(1/G) + (1/h_0)]\}. \tag{38}$$

Equation (37) has two real roots for $|m_0| \leqq 1$, one of which is of course equal to 1. Denoting the other root by m^*, we can find that

$$0 < m^* \leqq (1/2), \tag{39}$$

and m^* tends to (1/2) for $a = h_0/H_0 \to 0$. In fact, m^* is generally very close to (1/2) which is coincident with m for plane-strain state of $\epsilon_{22} = 0$. Eventually the critical condition for the onset of breakage is summed up as follows:

$$\begin{aligned} &A = 0 \quad \text{for} \quad m^* \leqq m \leqq 1, \\ &C = -2\sqrt{A \cdot E} \quad \text{for} \quad -1 \leqq m < m^*. \end{aligned} \tag{40}$$

When A becomes equal to 0, from eqn (31), g_2 gets equal to 0, which means the local neck band lies in parallel with the 2-axis, i.e. $\psi = 0$ in Fig. 1, where the direction of the neck band is undefinite for $m = 1$, because the critical condition reduces to $A = C = E = 0$ for $m = 1$. On the other hand, for $m = m^*$, $A = C = 0$ and $E \neq 0$ hold at the critical state and thus $g_2 = 0$. And, for $-1 \leqq m < m^*$, the direction of the local neck band is determined from eqns (31) and (40)). Eventually we have the following formulae:

$$\psi = 0, \quad \theta = \pi/2 \quad \text{for} \quad m^* \leqq m < 1, \tag{41}$$

$$\psi = \tan^{-1}(\sqrt[4]{A/E}) \quad \text{for} \quad -1 \leqq m < m^*. \tag{42}$$

Now we can derive the breakage condition in its concrete form from eqns (32),

(33), (39) and (40) as follows:

(i) $m^* \leqq m \leqq 1$;

$$\sigma_1[(1/G) + (1/h_0)] = 4(1 + b(2m - 1)^2/\{4h_0(1 - m + m^2)[(1/G) + (1/H_0)]\}). \tag{43}$$

(ii) $-1 \leqq m < m^*$;

$$\sigma_1[(1/G) + (1/h_0)]' = f_1/(f_2 + \sqrt{f_3});$$

$$\begin{aligned}
f_1 &= 18a_{33}b/[h_0(1 - m + m^2)] - 2\sigma^{*2}\{1 + a_{33}b(2m - 1)^2/[4h_0(1 - m + m^2]\} \\
&\quad \times \{1 + a_{33}b(2 - m)^2/[4h_0(1 - m + m^2)]\}, \\
f_2 &= 3a_{33}b(1 + m)/\{2h_0(1 - m + m^2)\} - (\sigma^*/2)\{1 + a_{33}b(2 - m) \\
&\quad \times (2m - 1)/[4h_0(1 - m + m^2)]\} \\
&\quad - (\sigma^{*2}/4)(1 + m)\{1 + a_{33}b(4m^2 - 7m + 4)/[4h_0(1 - m + m^2)]\}, \\
f_3 &= \{a_{33}b/[4h_0(1 - m + m^2]\}\cdot(9 - 3(1 - m + m^2)\sigma^{*2} \\
&\quad + (1 + m)[3\sigma^* - (3/4)(1 - m)^2\sigma^{*3} \\
&\quad + (3/16)(1 - m)^2(1 + m)\sigma^{*4}] \\
&\quad + \{a_{33}b(1 + m)/[h_0(1 - m + m^2)]\}\cdot[9(1 + m) \\
&\quad - (3/2)\sigma^*(2 - m)(2m - 1) - (3/4)\sigma^{*2}(1 + m)(4m^2 - 7m + 4) \\
&\quad + (3/8)\sigma^{*3}(1 - m)^2(2 - m)(2m - 1) \\
&\quad + (3/16)\sigma^{*4}(1 - m)^2(1 + m)(1 - m + m^2)]),
\end{aligned} \tag{44}$$

$$\sigma^* = \sigma_1/a_{33}.$$

By making use of eqns (43) and (44), we can calculate and draw the FLD (forming limit-strain diagram; or FLC, forming limit-strain curve) for arbitrary metal sheet subjected to proportional loadings.

In the following numerical examples, we use the N-th power hardening law for materials tested. Then we can use the following approximate relations:

$$\begin{aligned}
&h_0 \fallingdotseq N(\bar{\sigma}/3\bar{\epsilon}), \qquad H_0 \fallingdotseq (1/3g)\,(\bar{\sigma}/\bar{\epsilon}), \qquad H_0/h_0 \fallingdotseq 1/gN, \\
&\bar{\sigma}/H_0 \fallingdotseq 3g\bar{\epsilon}, \qquad \bar{\sigma}/h_0 \fallingdotseq 3\bar{\epsilon}/N \qquad (g\text{: some factor}).
\end{aligned} \tag{45}$$

And the strain ratio $n = \epsilon_2/\epsilon_1$ has the following relation with m:

$$m = (2n + 1)/(2 + n),$$

and thus, corresponding to m^*, we can define $n^* = (2m^* - 1)/(2 - m^*)$ which follows from this equation, where $\epsilon_1 = \epsilon_{11}$ and $\epsilon_2 = \epsilon_{22}$.

Finally, we have assumed the Mises material extended to that with vertex effect so far. We can derive various formulae for the material with anisotropy expressed by Hill's quadratic yield function[10] or by the author's fourth-order yield function[11] by the similar procedure as above as well.

4. FORMULAE FOR $-1 \leqq m < m^*$

Neglecting $(1/G)$ in comparison with $(1/h_0)$, from eqn (42), we obtain the following formula for the angle ψ:

$$\psi = \tan^{-1}(\sqrt[4]{A/E}),$$

$$A/E = \frac{[3(H_0/h_0)n^2 + (2+n)^2 - (\sigma_1/h_0)(1+n+n^2)]}{\{3(H_0/h_0) + (1+2n)^2 - (\sigma_1/h_0)[(2n+1)/(2+n)](1+n+n^2)\}} \times \frac{[2(2+n) + (\sigma_1/H_0)(1-n)]}{[2(2+n) - (\sigma_1/H_0)(1-n)]} \tag{46}$$

Particularly, for the materials with N-th power hardening law, we have

$$A/E = \frac{[(3/gN)n^2 + (2+n)^2 - (2/N)(2+n)(1+n+n^2)\epsilon_1]}{[(3/gN) + (1+2n)^2 - (2/N)(1+2n)(1+n+n^2)\epsilon_1]} \times \frac{[1+g(1-n)\epsilon_1]}{[1-g(1-n)\epsilon_1]}; \qquad \epsilon_1 = \epsilon_{11}. \tag{47}$$

Figure 2 (numerical example), illustrates the relation between $\theta = (\pi/2) - \psi$ and N-value for $n = -0.5$ (uniaxial tension) and -1 (tension-compression) calculated from eqn (47), where, for convenience of comparison with S–R's theory, the factor g is kept to be 0.5, which means the angle Θ_0 (= the half angle of the point-wise vertexed subsequent loading surface at the loading point) is kept constant, though this assumption is not compatible with eqn (10). We should note that S–R's curve corresponds to that for $g = 1$[9]. Hill's theory[4] gives constant θ as illustrated in the figure. S–R's curves show a too much variation in θ. Therefore we can say that the value of g is generally between 0 and 1. [Note that, if eqn (10) is adopted, $gN = \cos\Theta_0/(1+\cos\Theta_0) \doteqdot \rho\bar{\epsilon}^2/(1+\rho\bar{\epsilon}^2)$, and thus g is generally a variable.]

Next, from eqn (44), we can obtain the following formulae of the limiting major strain $(\epsilon_1)_{cr}$:

(i) $m = -1$ $(n = -1)$;

$$(\epsilon_1)_{cr}/N \doteqdot \frac{3\bar{h} - \sigma^{*2}[1 + (3\bar{h}/4)]^2}{-(\sigma^*/2)[1 - (3\bar{h}/4)] + \sqrt{[(3\bar{h}/4)(1-\sigma^{*2})]}}, \tag{48}$$
$$\bar{h} \doteqdot (1/gN) - 1, \qquad \sigma^* \doteqdot 2g\epsilon_1; \qquad \epsilon_1 = (\epsilon_1)_{cr}.$$

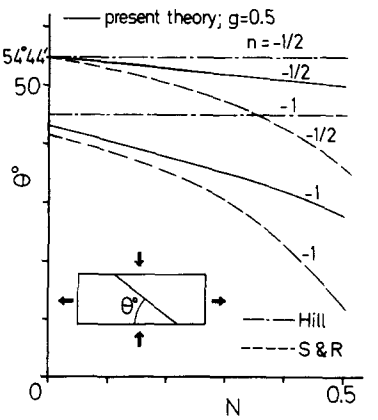

Fig. 2. Relation between N-value and direction of localized necking band (calculation).

(ii) $m = 0$ $(n = -0.5)$;

$$(\epsilon_1)_{cr}/N \doteqdot \frac{6\bar{h} - (1/6)\sigma^{*2}(1 + \bar{h})(4 + \bar{h})}{(1/4)\{6\bar{h} - \sigma^*(2 - \bar{h}) - \sigma^{*2}(1 + \bar{h})\} + \sqrt{\{(3/4)\bar{h}(1 + \bar{h})[3 + \sigma^* - \sigma^{*2} - (1/4)\sigma^{*3} + (1/16)\sigma^{*4}]\}}}, \tag{49}$$

$$\bar{h} \doteqdot (1/gN) - 1, \qquad \sigma^* = 3g\epsilon_1; \qquad \epsilon_1 = (\epsilon_1)_{cr}$$

We should note that both of these expressions involve $(\epsilon_1)_{cr}$ on both sides and thus these are not the explicit formulae of it. These will be used in the numerical examples given below.

5. FORMULAE OF LIMITING STRAIN FOR $m^* \leqq m \leqq 1$

By making use of eqn (43), we can derive the following formulae of the limiting major strain $(\epsilon_1)_{cr}$ as the functions of strain ratio n.

5.1 *Formulae for the case of constant* Θ_0

This case is equivalent to that where g is kept constant.

(i) *Mises material with* g = *1:*

$$(\epsilon_1)_{cr} \doteqdot [3n^2 + N(2 + n)^2]/[2(2 + n)(1 + n + n^2)]. \tag{50}$$

This is coincident with the formula due to S–R's theory or Hill's local necking condition with J_2-deformation theory[9].

(ii) *Material with normal anisotropy* $\bar{r}$: This is the case where anisotropy expressed by Hill's quadratic yield function is considered with the assumption of in-plane isotropy[10], where $\bar{r}$ denotes the in-plane average of r-value which is the ratio (breadth strain)/(thickness strain) in uniaxial tensile test and usually considered constant with deformation.

$$(\epsilon_1)_{cr} \doteqdot (N/2)((2 + an)\{2 + [(2a - 1) + (1 - a)gN]n\} + (4 - a^2)n^2/gN)/[(2 + an)(1 + n + n^2)], \tag{51}$$

$$a = 2\bar{r}/(1 + \bar{r}).$$

(iii) *Material with normal anisotropy* $\bar{r}$ *and* $\bar{X}$: This is the case where anisotropy expressed by the author's fourth-order yield function is considered with the assumption of in-plane isotropy[11], where $\bar{X}$ denotes the ratio (yield strength for equibiaxial tension σ_b)/(in-plane average of yield strength for uniaxial tension σ_u) at the same level of plastic work.

$$\begin{aligned}
(\epsilon_1)_{cr} &\doteqdot [4NM_1^*M/F(m)][1 + (1/8)(1 - gN)(2m - 1)(M_2^*/M) + (1/16gN)(1 - gN)^2M_2^{*2}/\sqrt{M^3}],\\
A_2 &= -4\bar{r}/(1 + \bar{r}), \qquad A_3 = (1/\bar{X}^4) - 2(1 + A_2),\\
M &= 1 + m^4 + A_2(m + m^3) + A_3m^2,\\
M_1^* &= 4 + 3A_2m + 2A_3m^2 + A_2m^3,\\
M_2^* &= A_2 + 2A_3m + 3A_2m^2 + 4m^3,\\
F(m) &= (16 + 4A_2 + A_2^2)(1 + m^6) + (24A_2 + 3A_2^2 + 4A_2A_3 + 8A_3)(m + m^5) + (12A_2 + 15A_2^2 + 8A_2A_3 + 4A_3^2 + 16A_3)(m^2 + m^4) + (16 + 16A_2 + 10A_2^2 + 24A_2A_3 + 4A_3^2)m^3,\\
n &= M_2^*/M_1^*.
\end{aligned} \tag{52}$$

5.2 *Formulae for the case where Θ_0 is variable with deformation*

Two cases are considered, one of which is that where Θ_0 is given by eqn (10), and the other is that where the loading surface possesses a certain amount of initial vertex which may represent a certain ambiguity of initial yielding which is usually common in mild-quality metal sheets. Only Mises material with vertex effect is considered.

(i) $\Theta_0 = (\pi/2) - \rho\bar{\epsilon}^2$; $gN \doteqdot \rho\bar{\epsilon}^2/(1 + \rho\bar{\epsilon}^2)$:

$$(\epsilon_1)_{cr} = x, \quad x^3 - bx^2 - c' = 0,$$
$$b = 2N/(2 + n), \quad c' = 2.25Nn^2/[2\rho(2 + n)(1 + n + n^2)^2], \tag{53}$$
$$\rho \doteqdot 0.04167N/(x_1^3 - 0.6667Nx_1^2), \quad x_1 = [(\epsilon_1)_{cr}]_{n=1}.$$

(ii) $\Theta_0 = \psi_0 - \rho\bar{\epsilon}^2$; $gN = \cos\Theta_0/(1 + \cos\Theta_0)$:

$$(\epsilon_1)_{cr} = x, \quad x^3 - bx^2 + ex - c = 0,$$
$$b = 2N/(2 + n), \quad e = 0.750 \cot\psi_0/[\rho(1 + n + n^2)],$$
$$c = 0.750N\{3n^2 + \cos\psi_0\,[3n^2 + (2 + n)^2]\}/\{\rho \sin\psi_0\{2(2 + n)(1 + n + n^2)^2]\}, \tag{54}$$
$$\rho \doteqdot [0.01389N(3 \operatorname{cosec}\psi_0 + 12 \cot\psi_0) - 0.25 \cot\psi_0 x_1]/(x_1^3 - 0.6667Nx_1^2),$$
$$\cos\psi_0 = 0.5N/(1 - 0.5N), \text{ (say)},$$

where, for convenience, ψ_0 is given as that for Θ_0 which is calculated by putting $g = 0.5$.

In the above two formulae (53) and (54), the newly introduced material constant ρ in our plastic constitutive equation (1) is determined in the manner that the theoretical value of $(\epsilon_1)_{cr}$ for $m = n = 1$ is coincident with that by the experiment. Of course, there may exist other various methods to determine ρ other than this method.

6. EXAMPLES OF FLD

6.1 *FLD for constant* g

Figure 3 illustrates examples of FLD for $N = 0.5$ and 0.22 with constant g calculated from eqns (50)–(52), where $N = 0.22$ represents a kind of rimmed steel sheet at hand.

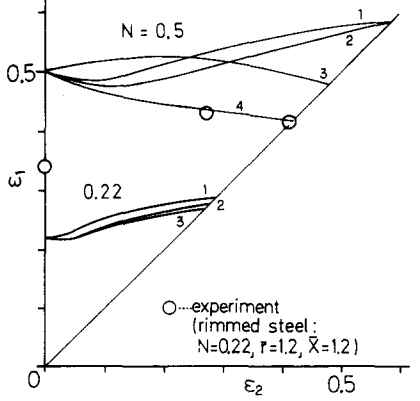

Fig. 3. Numerical example of FLD (constant vertex angle). $N = 0.5$: 1—isotropy with $g = 0.5$; 2—normal anisotropy with fourth-order yield function, $\bar{r} = 2.0$, $\bar{X} = 1.0$, $g = 0.5$; 3—normal anisotropy with fourth-order yield function, $\bar{r} = 1.0$, $\bar{X} = 1.5$, $g = 0.5$; 4—isotropy with $g = 1.0$ (S–R curve). $N = 0.22$; 1—normal anisotropy with fourth-order yield function, $\bar{r} = \bar{X} = 1.2$, $g = 0.75$; 2—S–R curve; 3—normal anisotropy with quadratic yield function, $\bar{r} = 1.2$, $g = 1.0$ (N, $\bar{r}$, $\bar{X}$ are measured values of a rimmed steel).

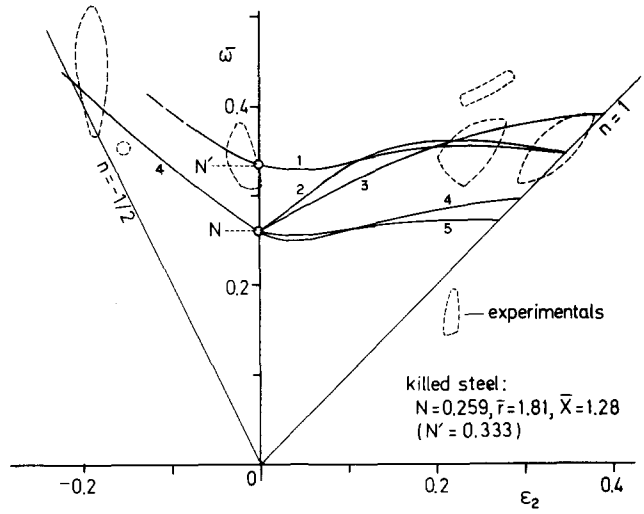

Fig. 4. Theoretical FLDs and experimentals, a killed steel (KS). 1—$\Theta_0 = \psi_0 - \rho\bar{\epsilon}^2$, $\psi_0 = 78°$ 29′, $\rho = 0.5$; 2—$\Theta_0 = (\pi/2) - \rho\bar{\epsilon}^2$, $\rho = 0.5$; 3—normal anisotropy with fourth-order yield function, $\bar{r} = 1.81$, $\bar{X} = 1.28$, $g = 0.5$; 4—S–R curve; 5—normal anisotropy with quadratic yield function, $\bar{r} = 1.81$, $g = 0.5$ (N' is used for the curve 1 instead of N).

From the curves for $N = 0.5$, it is found that the effect of $\bar{r}$ is little, and that $\bar{X}$ greater than unity raise the limiting strain for the strain ratio between 0 and 1. A defect of FLD due to S–R theory is that it is apt to give a too low value of the limiting strain for the same range of strain ratio. Therefore, we can say that it may be one method to improve theoretical FLD to take $\bar{X}$ into consideration. Of course, as seen in the figure, the effect of the value of g is most prominent.

All the theoretical curves for $N = 0.22$ locate at the lower site than the experimental plots which are the averages of the scattering experimental data shown later in Fig. 5.

6.2 *FLDs of various commercial metal sheets*

The author and co-workers[12] reported in another paper FLDs of various commercial metal sheets such as an aluminium-killed steel (KS), a rimmed steel (RS), soft aluminium (Al-0), half-hard aluminium (Al-½H), a quarter-hard copper (Cu-¼H), and a

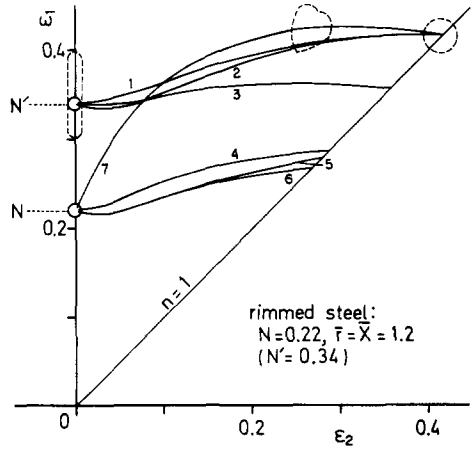

Fig. 5. Thoretical FLDs and experimentals, a rimmed steel (RS). 1—normal anisotropy with fourth-order yield function, $\bar{r} = \bar{X} = 1.2$, $g = 0.523$; 2—$\Theta_0 = \psi_0 - \rho\bar{\epsilon}^2$, $\psi_0 = 78°$ 11′, $\rho = 0.1365$; 3—normal anisotropy with fourth-order yield function, $\bar{r} = \bar{X} = 1.2$, $g = 0.75$ (N' instead of N is used for the curves 1, 2 and 3); 4—the same as 3 except N; 5—S–R curve; 6—normal anisotropy with quadratic yield function; $\bar{r} = 1.2$, $g = 1.0$; 7—$\Theta_0 = (\pi/2) - \rho\bar{\epsilon}^2$, $\rho = 0.195$.

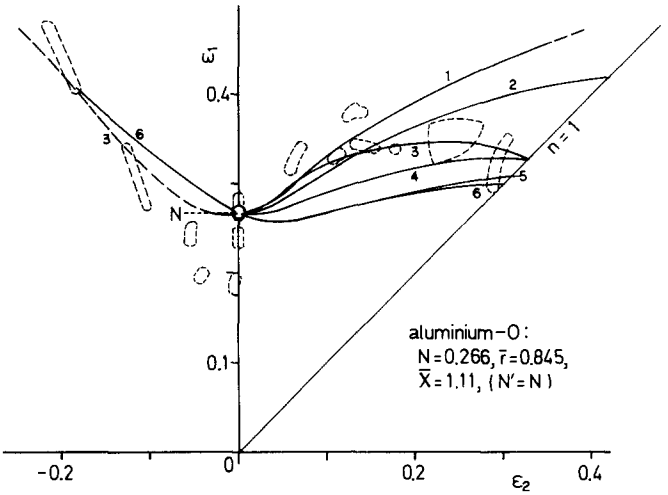

Fig. 6. Theoretical FLDs and experimentals, a soft aluminium (Al-0). 1—normal anisotropy with fourth-order yield function, $\bar{r} = 0.845$, $\bar{X} = 1.11$, $g = 0.4$; 2—the same as 1 except $g = 0.5$; 3—$\Theta_0 = (\pi/2) - \rho\bar{\epsilon}^2$, $\rho = 0.667$; 4—the same as 1 except $g = 0.75$; 5—normal anisotropy with quadratic yield function, $\bar{r} = 0.845$, $g = 1.0$; 6—S–R curve.

quarter-hard (60/40) brass (Bs-$\frac{1}{4}$H), with thickness of 0.8 mm. They all have the experimental plots both in the range $\epsilon_2 \leqq \epsilon_1$ and $\epsilon_2 \geqq \epsilon_1$ because of in-plane anisotropy, and a considerable amount of scattering of them. They are replotted in Figs. 4–9 in the manner that all the plots in the range $\epsilon_2 > \epsilon_1$ are shifted to the corresponding positions in the range $\epsilon_2 \leqq \epsilon_1$ neglecting in-plane anisotropy, and all the plots so obtained are encircled by dotted lines to show their scattering feature.

On the other hand, the corresponding theoretical FLDs are also drawn in each figure for various possible conditions noted below the figures. The experimental data in Fig. 10 are replotted from Tadros and Mellor's paper[13] which are for a soft (70/30) brass (Bs-0).

Now the theoretical limiting strain $(\epsilon_1)_{cr}$ for $n = 0$ (i.e. plane-strain state) is equal to the value of N itself for all the formulae (51)–(54). However, N-values adopted here are all determined by uniaxial tensile test taking the in-plane averages. And the range of strain in determination of N is rather small when it is compared with the limiting strain, especially in the range of $0 \leqq n \leqq 1$. Therefore the adopted value of N is not

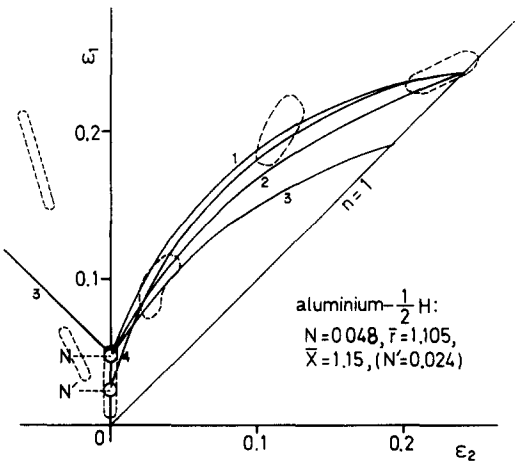

Fig. 7. Theoretical FLDs and experimentals, a half-hard aluminium (Al-$\frac{1}{2}$H). 1—$\Theta_0 = \psi_0 - \rho\bar{\epsilon}^2$, $\psi_0 = 88°\ 35'$, $\rho = 0.0602$; 2—isotropy with $g = 0.7716$ ($\Theta_0 = 87°\ 48'$); 4—$\Theta_0 = \psi_0 - \rho\bar{\epsilon}^2$, $\psi_0 = 89°\ 18'$, $\rho = 0.02472$ (N' instead of N is used for the curve 4); 3—S–R curve.

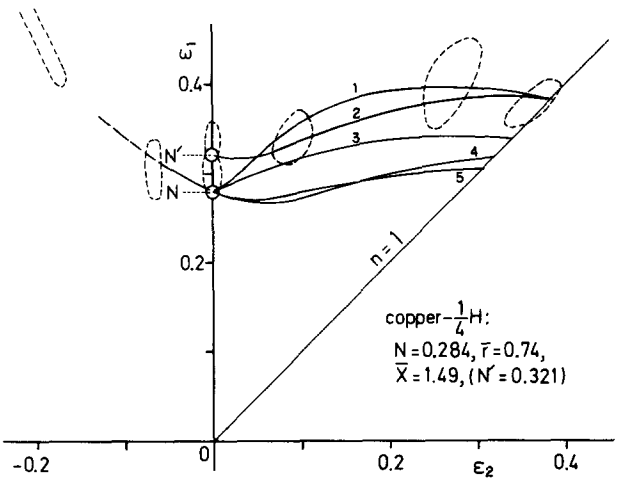

Fig. 8. Theoretical FLDs and experimentals, a quarter-hard copper (Cu-$\frac{1}{4}$H). 1—$\Theta_0 = (\pi/2) - \rho\bar{\epsilon}^2$, $\rho = 0.4051$; 2—$\Theta_0 = \psi_0 - \rho\bar{\epsilon}^2$, $\psi_0 = 78°\ 59'$, $\rho = 0.2176$ (N' instead of N is used for the curve 2); 3—normal anisotropy with fourth-order yield function, $\bar{r} = 0.74$, $\bar{X} = 1.49$, $g = 0.5$; 4—normal anisotropy with quadratic yield function, $\bar{r} = 0.74$, $g = 1.0$; 5—S–R curve.

necessarily appropriate. In fact, as seen in the figures, denoting $[(\epsilon_1)_{cr}]_{n=0}$ by N', there exist materials whose N' is comparatively greater than N (KS, RS), less than N (Al-$\frac{1}{2}$H, Bs-0), or approximately equal to N (other metals). The theoretical curves due to eqn (53) or (54) agree fairly well with the experimentals, even for the materials whose N' has a great difference with N, though those due to other formulae show poor agreement with the experimentals. Only one exception is Bs-0. Even for the materials whose N' deviates much from N, if N' is used instead of N, the theoretical curves due to eqn (53) or (54) are almost completely coincident with the experimentals, which is particularly seen for Bs-0.

All the S–R curves show very poor agreement with the experimentals in spite of large scattering of them. All the figures demonstrate that FLDs due to our constitutive equation (1) together with Θ_0 expressed by eqn (10), or in eqn (54), can predict the experiments much better than those due to S–R's theory.

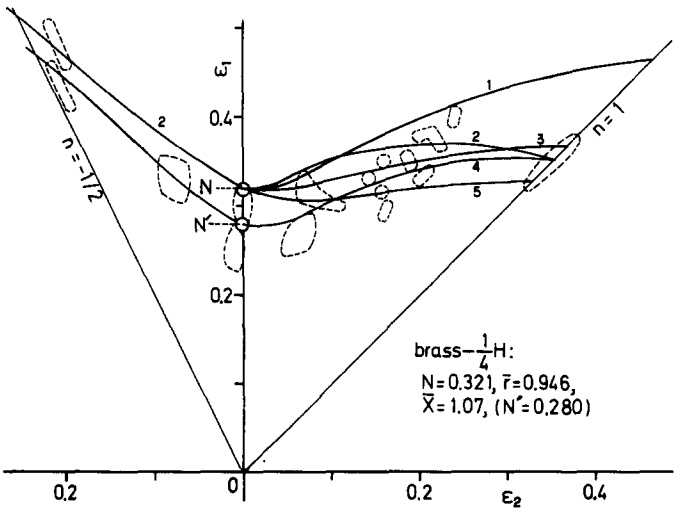

Fig. 9. Theoretical FLDs and experimentals, a quarter-hard brass (Bs-$\frac{1}{4}$H). 1—normal anisotropy with fourth-order yield function, $\bar{r} = 0.946$, $\bar{X} = 1.07$, $g = 0.5$; 2—$\Theta_0 = (\pi/2) - \rho\bar{\epsilon}^2$, $\rho = 0.772$; 3—the same as 1 except $g = 0.75$; 4—$\Theta_0 = \psi_0 - \rho\bar{\epsilon}^2$, $\psi_0 = 80°\ 38'$, $\rho = 0.2394$ (N' instead of N is used for the curve 4); 5—normal anisotropy with quadratic yield function, $\bar{r} = 0.946$, $g = 1.0$; S–R curve almost coincides with 5.

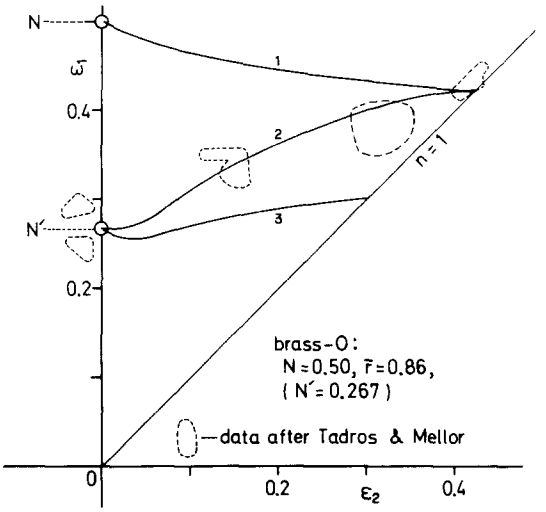

Fig. 10. Theoretical FLDs and experimentals, a soft brass (Bs-0). 1—S–R curve ($\Theta_0 \doteqdot 90°$); 2—$\Theta_0 = \psi_0 - \rho\bar{\varepsilon}^2$, $\psi_0 = 81° 08'$, $\rho = 0.03423$; 3—S–R curve ($\Theta_0 = 68° 38'$) (N' instead of N is used for the curves 2 and 3).

Table 1. The half angle Θ_0 of vertexed cone of subsequent loading surface at onset of breakage (calculation)

Material \ Strain ratio	1—0
KS	70°—85°
RS	72°—88°
Al–O	73°—85°
Al–$\frac{1}{2}$H	87°—89°
Cu–$\frac{1}{4}$H	73°—86°
Bs–$\frac{1}{4}$H	70°—82°
Bs–O	79°—80°

Table 1 shows the values of Θ_0 (the half angle of the point-wise vertexed cone of the subsequent loading surface at the loading point) at the onset of breakage of the all materials tested here when eqn (53) or (54) is used. Note that $\Theta_0 = (\pi/2)$ means no vertex, i.e. the subsequent loading surface is always smooth. As found from this table, even at the time of breakage, Θ_0 remains in the range of 70°–90°. That is, our constitutive equation predicts that any metal sheet will break with rather dull vertex of the subsequent loading surface and thus, for continuing deformation of ordinary amount, the evolution of the vertex is little. This can explain that it is difficult, as reported so far by many workers, to check directly the vertex-formation on the subsequent loading surface by the usual method of determination of the surface at the level of small strain. Of course, even if its evolution is not prominent, the pointed vertex on the subsequent loading surface at the loading point plays a decisive role in inducing local necking or breakage.

7. CONCLUSION

The elastoplastic constitutive equation developed in the previous two papers of this series is applied to determination of FLD (forming limit-strain diagram) of metal sheets subjected to proportional loadings. First, the constitutive equation is reduced to that for plane stress state, and then the formulae of the limiting strain or stress and the direction of the local neck band are derived by making use of localized-type bi-

furcation condition as the breakage condition. The formulae take different forms for $-1 \leqq m \leqq m^*$ and $m^* \leqq m \leqq 1$, where m denotes the stress ratio σ_2/σ_1 and $|m| \leqq 1$. For $m^* \leqq m \leqq 1$, the neck band lies perpendicular to 1-axis (the major stress axis). Generally, $0 < m^* \leqq 0.5$ holds and m^* is very close to 0.5. The formulae for the case where normal anisotropy (in-plane isotropy) expressed by Hill's quadratic yield function or by the author's fourth-order yield function are also given. For several commercial sheet metals, theoretical FLDs are determined and illustrated to compare with the experiments. It is found that FLD due to Stören and Rice's theory gives poor quantitative prediction, that FLD due to our theory, which allows Θ_0 (= the half angle of the point-wise vertexed subsequent loading surface at the loading point) to reduce with deformation, gives a good quantitative prediction, and that the latter FLD is almost completely coincident with the corresponding experimental one if N' [= limiting major strain $(\epsilon_1)_{cr}$ at strain ratio $n = 0$] is adopted as the strain-hardening exponent instead of N which is determined by uniaxial tensile test.

It is also pointed out that the value of Θ_0 remains within the range of 70°–90° throughout all the materials tested here even at the time of breakage and thus the evolution of the vertex of the subsequent loading surface is very dull when stable deformation continues at lower strain level. However, if such vertex-formation were not assumed to occur, the localized bifurcation and thus breakage cannot take place at reasonable stress or strain level.

REFERENCES

1. M. Gotoh, A class of plastic constitutive equations with vertex effect—I. General theory. *Int. J. Solids Structures* **21**, 1101 (1985).
2. M. Gotoh, A class of plastic constitutive equations with vertex effect—II. Discussions on the simplest form. *Int. J. Solids Structures* **21**, 1117 (1985).
3. H. W. Swift, Plastic instability under plane stress. *J. Mech. Phys. Solids* **1**, 1 (1952).
4. R. Hill, On discontinuous plastic states, with special reference to localized necking in thin sheets. *J. Mech. Phys. Solids* **1**, 19 (1952).
5. Z. Marciniak and K. Kuczynski, Limit strains in the processes of stretch-forming sheet metals. *Int. J. Mech. Sci.* **9**, 609 (1967).
6. R. Sowerby and J. L. Duncan, Failure in sheet metal in biaxial tension, *Int. J. Mech. Sci.* **13**, 217 (1971).
7. A. K. Tadros and P. B. Mellor, Some comments on the limit strains in sheet metal stretching. *Int. J. Mech. Sci.* **17**, 203 (1975).
8. A. Parmar and P. B. Mellor, A new model for the prediction of instability and limit strains in thin sheet metal. *Int. J. Mech. Sci.* **19**, 389 (1977).
9. S. Stören and J. R. Rice, Localized necking in thin sheets. *J. Mech. Phys. Solids* **23**, 42 (1975).
10. R. Hill, *The Mathematical Theory of Plasticity*, p. 317. Oxford University Press, New York (1950).
11. M. Gotoh, A theory of plastic anisotropy based on a yield function of fourth order (plane stress state)—I and II, *Int. J. Mech. Sci.* **9**, 505, 513 (1977).
12. Y. Sato, M. Gotoh and A. Morikawa, Forming limit strains of sheet metals subjected to biaxial tensions. *Trans. Jpn Soc. Mech. Engrs., Ser. A* (in Japanese) **47**, 1183 (1981).
13. A. K. Tadros and P. B. Mellor, An experimental study of the in-plane stretching of sheet metal. *Int. J. Mech. Sci.* **20**, 121 (1978).